Consistent Distributed Track Fusion Under Communication Constraints

Robin Forsling, Zoran Sjanic, Fredrik Gustafsson and Gustaf Hendeby

Forsling, R., Sjanic, Z., Gustafsson, F., Hendeby, G., (2019), Consistent Distributed Track Fusion Under Communication Constraints, *Proceedings of the 22nd International Conference on Information Fusion (FUSION)*.

Consistent Distributed Track Fusion Under Communication Constraints

Robin Forsling*†, Zoran Sjanic*†, Fredrik Gustafsson*, and Gustaf Hendeby*
* Dept. of Electrical Engineering, Linköping University, Linköping, Sweden
e-mail: {firstname.lastname}@liu.se
† Saab AB, Linköping, Sweden
e-mail: {firstname.lastname}@saabgroup.com

***Abstract*—This paper addresses the problem of retrieving consistent estimates in a distributed network where the communication between the nodes is constrained such that only the diagonal elements of the covariance matrix are allowed to be exchanged. Several methods are developed for preserving and/or recovering consistency under the constraints imposed by the communication protocol. The proposed methods are used in conjunction with the *covariance intersection* method and the estimation performance is evaluated based on information usage and consistency. The results show that among the proposed methods, consistency can be preserved equally well at the transmitting node as at the receiving node.**

***Index Terms*—distributed estimation, track fusion, communication constraints, covariance intersection, consistency, consistency preservation**

I. Introduction

Target tracking using standard tracking sensors, *e.g.*, radar, lidar, sonar, or *infrared search and track* (IRST), is a relatively mature area, using centralized methods with access to the obtained measurements. The *multiple-hypothesis tracker* (MHT), or more recently different method based on *finite state statistics* (FISST), have proven to provide reliable estimates of the state of the targets in the tracking volume. This works well within sensor platforms and small well defined sensor networks, but does not scale well to several platforms or larger *ad hoc* networks. These situations often call for distributed solutions, where the computations are distributed and performed in each individual platform or sensor node, and state estimates are communicated between the nodes to obtain joint estimates.

Distributed tracking solutions have several practical benefits compared to centralized fusion. They are less sensitive to lost nodes or connections as there is not only a single central node that performs the tracking, the computational complexity is spread among the different nodes, and it is easy to add and remove nodes on the fly. However, these benefits come with drawbacks. In general, distributed solutions have to make approximations making them suboptimal. Further, without proper care taken, there is a risk to double count information resulting in inconsistent estimates. Preserving consistency of the estimates is one of the main concerns of any distributed tracking system as inconsistency can potentially lead to diverging estimates. Consistency in this context is defined as [1]

$$\mathbf{P} - E[\tilde{\mathbf{x}}\tilde{\mathbf{x}}^{\mathsf{T}}] \succeq 0, \tag{1}$$

where $\tilde{\mathbf{x}} = \mathbf{x} - \hat{\mathbf{x}}$ is the deviation of the estimated state from the true state $\mathbf{x}$, $\succeq$ denotes positive semi-definiteness, and $\mathbf{P}$ is the approximation of the covariance of the estimate. Furthermore, in order to save bandwidth many practical solutions limit the information communicated between nodes, complicating the estimation process.

Keeping track of all cross-correlations between the estimates in the different nodes (see [2] for details), it is possible to compensate for these when fusing the estimates using Bar-Shalom-Campo formulas [3, 4]. In practice, it quickly becomes intractable to keep track of all cross-correlations, therefore methods that are robust to cross-dependencies have been developed. Information can be decorrelated using different techniques [5–7] or the cross-correlations themselves can be modeled as in [8, 9].

The *covariance intersection* (CI, [1, 10]) method is a popular method used to fuse (possibly) correlated estimates. If the fused estimates themselves are consistent, the fused estimate will be consistent too. This makes the CI method quite conservative. A number of similar methods exist; *e.g.*, *largest ellipsoid* (LE, [11]), *ellipsoidal intersection* (EI, [12, 13]), *safe fusion* (SF, [14]) which is identical to EI but derived in a different way, which are all less conservative but lack consistency guarantees. The *inverse covariance intersection* (ICI, [15, 16]), is a relatively new method, guaranteeing consistency under relatively mild assumptions. The effectiveness of these methods have previously been studied, see, *e.g.*, [17]. A geometrical approach, using Minkowski sums, for deriving an upper bound on the covariance of fused estimate is studied in [18].

In practice, communicating both the state estimate and the full covariance is needed in order to be certain of providing consistent estimates. However, this requirement might be hard to fulfill given the available bandwidth. The literature on how to deal with this is limited. The *covariance union* (CU, [19]) method which is designed to provide a consistent result when fusing two estimates, of which only one is guaranteed to be

This work has been supported by the Industry Excellence Center LINK-SIC funded by The Swedish Governmental Agency for Innovation Systems (VINNOVA) and Saab AB, and by the project Scalable Kalman filters funded by the Swedish Research Council (VR).

consistent, is one exception. Though powerful, CU is overly conservative if it is known which estimate is consistent, as is in this paper.

This paper derives consistent estimates for the special case where, due to bandwidth limitations, only the state estimate and the diagonal of the covariance matrix is communicated between nodes. In this case, where the communicated estimates are prone to be inconsistent and the local estimate can be assumed to be consistent, the CU is overly conservative whereas CI cannot guarantee consistency. Five different new methods are proposed to handle this case. Three methods in which the communicated diagonal covariance matrix are compensated before being communicated, and two which can be implemented in the receiving node. The benefit of the latter is that it can be implemented without modifying existing sensor nodes and communication protocols. A simulation study is performed to compare the proposed solutions with: i) the case when estimates from other nodes are ignored; ii) a centralized filter, and; iii) a naïve filter disregarding any cross-correlations between estimates.

The paper is organized as follows. Sec. II defines the problem and sets the notation. The fusion methods used are described in Sec. III, and the proposed methods to deal with the inconsistent estimates are derived in Sec. IV. Sec. V specifies the simulation scenario, the metrics used for the evaluation and presents the results. Concluding remarks are given in Sec. VI.

II. Problem Statement

In the normal setting the distributed fusion problem is to fuse a local consistent estimate $(\hat{\mathbf{x}}_1, \mathbf{P}_1)$ at node 1 with consistent estimates $(\hat{\mathbf{x}}_i, \mathbf{P}_i)$ from node i being robust to potential cross-correlations between the estimates. The extension studied in this paper is the case when only $(\hat{\mathbf{x}}_1, \mathbf{P}_1)$ is consistent and for $i \neq 1$, due to communication limitations, $\mathbf{P}_i$ is approximated with $\mathbf{D}_i$ containing only the diagonal elements of $\mathbf{P}_i$.

We here denote the original and assumed consistent estimate by the pair $(\hat{\mathbf{x}}, \mathbf{P})$ where $\hat{\mathbf{x}}$ is the state estimate and $\mathbf{P}$ the estimated covariance of $\hat{\mathbf{x}}$. The, in general inconsistent, estimate $(\hat{\mathbf{x}}, \mathbf{D})$ is obtained by approximating $\mathbf{P}$ by its diagonal entries. Without loss of generality node 1 will be assumed to be the local estimate and fusion node, for which the full covariance matrix $\mathbf{P}_1$ is known, and for the remaining estimates only the diagonal approximations $\mathbf{D}_i$ are available.

A. Network Aspects

The network considered is a distributed sensor network of dynamic nodes where each node has a suite of sensors, *e.g.* INS/GPS, tracking sensor(s), datalink, and is also capable of fusing sensor data. The datalink defines the network communication links and, as stated above, does not permit off-diagonal entries of the covariance matrix to be transmitted.

B. Implications of the Covariance Approximation

Any estimate where $\mathbf{P}$ is approximated by $\mathbf{R}$ is consistent if

$$\mathbf{R} - \mathbf{P} \succeq 0, \tag{2}$$

since $\mathbf{R}$ fulfilling (2) will automatically also fulfill (1). Approximating the full covariance matrix $\mathbf{P}$ by its diagonal version $\mathbf{D}$ will in general generate an inconsistent estimate. To exemplify this, consider $\mathbf{P}$ defined by

$$\mathbf{P} = \begin{bmatrix} p_{11} & p_{12} \\ p_{12} & p_{22} \end{bmatrix} \succeq 0, \tag{3}$$

with the diagonal approximation $\mathbf{D}$ given by

$$\mathbf{D} = \begin{bmatrix} p_{11} & 0 \\ 0 & p_{22} \end{bmatrix} \succeq 0. \tag{4}$$

The characteristic equation for the matrix on the left-hand-side of (2), with $\mathbf{D}$ replacing $\mathbf{R}$, is

$$\det[\lambda \mathbf{I} - (\mathbf{D} - \mathbf{P})] = \lambda^2 - p_{12}^2, \tag{5}$$

with the eigenvalues $\lambda = \pm p_{12}$, thus implying the matrix $(\mathbf{D} - \mathbf{P})$ is indefinite.

Note, consistency can be recovered for any inconsistent estimate by inflating the covariance but at the cost of decreasing the information content (recall that information is defined as $\mathbf{P}^{-1}$). This means that there will always be a compromise between information and consistency and both are indeed important properties. However, throughout this paper, consistency is regarded as the more important property.

III. Considered Fusion Methods

This section presents the fusion methods treated in this paper. Focus is on the CI algorithm but also the *Kalman filter* (KF) will be considered.

A. Local, Centralized and Naïve Filters

The KF will be used as a reference in this work. Results will be benchmarked against a *local KF* (LKF) with only access to local information and a *centralized KF* (CKF) with direct access to all measurements and full covariance from all the nodes. The LKF is used as an upper bound and the CKF is used as a lower bound. A *naïve KF* (nKF) neglecting any cross-correlations will be used to illustrate the problems of an overly optimistic estimator.

The fusion rule, for fusion of two estimates, is equivalent for LKF, CKF and nKF, and is given by

$$\mathbf{P}_f^{-1} = \mathbf{H}_1^\intercal \mathbf{P}_1^{-1} \mathbf{H}_1 + \mathbf{H}_2^\intercal \mathbf{P}_2^{-1} \mathbf{H}_2, \tag{6a}$$

$$\mathbf{P}_f^{-1} \hat{\mathbf{x}}_f = \mathbf{H}_1^\intercal \mathbf{P}_1^{-1} \hat{\mathbf{x}}_1 + \mathbf{H}_2^\intercal \mathbf{P}_2^{-1} \hat{\mathbf{x}}_2. \tag{6b}$$

The equation solves the *weighted least-squares* problem in case of independent estimates $(\hat{\mathbf{x}_1}, \mathbf{P}_1)$ and $(\hat{\mathbf{x}}_2, \mathbf{P}_2)$, and in fact constitutes the information form of the measurement update of the KF [20]. The measurement matrix $\mathbf{H}_i$ will differ depending on if $(\hat{\mathbf{x}}_i, \mathbf{P}_i)$ is a track estimate or a measurement. Equation (6) assumes the input tracks/measurements to be linear.

B. Covariance Intersection

The CI algorithm [1] fuses two or more consistent estimates $\hat{\mathbf{x}}_1, \hat{\mathbf{x}}_2, \ldots$ with unknown cross-correlations by taking convex combinations of the state estimates and their corresponding information matrices $\mathbf{P}_1^{-1}, \mathbf{P}_2^{-1}, \ldots$, respectively. The fusion rule, for fusion of two estimates, is given by [19]

$$\mathbf{P}_f^{-1} = \omega \mathbf{H}_1^\intercal \mathbf{P}_1^{-1} \mathbf{H}_1 + (1-\omega)\mathbf{H}_2^\intercal \mathbf{P}_2^{-1} \mathbf{H}_2, \tag{7a}$$

$$\mathbf{P}_f^{-1} \hat{\mathbf{x}}_f = \omega \mathbf{H}_1^\intercal \mathbf{P}_1^{-1} \hat{\mathbf{x}}_1 + (1-\omega)\mathbf{H}_2^\intercal \mathbf{P}_2^{-1} \hat{\mathbf{x}}_2, \tag{7b}$$

where $\hat{\mathbf{x}}_f$ is the fused state estimate, $\mathbf{P}_f$ the corresponding estimated covariance, and $\mathbf{H}_i$ is the measurement matrix projecting $\hat{\mathbf{x}}_f$ to $\hat{\mathbf{x}}_i$. If the state space of $\hat{\mathbf{x}}_i$ is the same as the state space of $\hat{\mathbf{x}}_f$, $\mathbf{H}_i$ reduces to the identity matrix. CI will provide a consistent fused estimate $(\hat{\mathbf{x}}_f, \mathbf{P}_f)$ for all values of the parameter $\omega \in [0,1]$ as long as both $(\hat{\mathbf{x}}_1, \mathbf{P}_1)$ and $(\hat{\mathbf{x}}_2, \mathbf{P}_2)$ are consistent [10]. In practice, ω is a tuning parameter that can be used to minimize an appropriate objective function, *e.g.* the trace or the determinant of $\mathbf{P}_f$.

The convex combination of the information matrices features the fact that, regardless of the cross-correlation between $\hat{\mathbf{x}}_1$ and $\hat{\mathbf{x}}_2$, the ellipsoid of the optimal covariance $\mathbf{P}_f$ will lie inside the intersection of the ellipsoids defined by $\mathbf{P}_1$ and $\mathbf{P}_2$. A covariance that encloses this intersection will therefore be consistent. CI produces consistent fused estimates $(\hat{\mathbf{x}}_f, \mathbf{P}_f)$ for the general case if the ingoing estimates $(\hat{\mathbf{x}}_1, \mathbf{P}_1), \ldots, (\hat{\mathbf{x}}_N, \mathbf{P}_N)$ are consistent [19]. The CI algorithm for fusion of N estimates is given in Alg. 1.

Algorithm 1 The CI algorithm [19]

Given N estimates $(\hat{\mathbf{x}}_i, \mathbf{P}_i)$ of the true state $\mathbf{x}$, with unknown cross-correlations, the fused estimate $(\hat{\mathbf{x}}_f, \mathbf{P}_f)$ is calculated as:

1) Find $\bar{\omega} = \begin{pmatrix}\omega_1 \ldots \omega_N\end{pmatrix}$ by solving the optimization problem given by

$$\begin{aligned} \underset{\bar{\omega}}{\text{minimize}} \quad & f(\mathbf{P}_f(\bar{\omega})) \\ \text{subject to} \quad & \mathbf{P}_f^{-1} = \sum_{i=1}^{N} \omega_i \mathbf{H}_i^\intercal \mathbf{P}_i^{-1} \mathbf{H}_i \\ & 0 \le \omega_i \le 1, \quad \sum_{i=1}^{N} \omega_i = 1, \end{aligned}$$

where the objective function f can for example be the trace or determinant. The measurement matrix $\mathbf{H}_i$ transforms $\hat{\mathbf{x}}_f$ to the state space of $\hat{\mathbf{x}}_i$.

2) The fused estimate is calculated as

$$\mathbf{P}_f = \left(\sum_{i=1}^{N} \omega_i \mathbf{H}_i^\intercal \mathbf{P}_i^{-1} \mathbf{H}_i \right)^{-1},$$

$$\hat{\mathbf{x}}_f = \mathbf{P}_f \sum_{i=1}^{N} \omega_i \mathbf{H}_i^\intercal \mathbf{P}_i^{-1} \hat{\mathbf{x}}_i.$$

As CI requires all the ingoing estimates to be consistent to guarantee consistency of the fused estimate, the algorithm cannot be directly applied when the diagonal covariance approximation is used. Methods for preserving consistency are presented in Sec. IV.

IV. Consistency Preservation of Diagonal Only Covariance Approximations

To allow for CI to be used correctly and consistently, the diagonal covariance approximation must be handled. In this section five methods for handling the diagonal covariance approximation are proposed. One method is an adaption of the CI algorithm and the other four methods belong to the class of covariance inflating (scaling) methods. Two of the scaling approaches originate from purely geometrical reasoning. The third scaling method is a non-uniform scaling based on solving an optimization problem and the last method relies on the relationship between diagonally dominant matrices, symmetry and positive semi-definiteness.

From a network communication point-of-view the consistency preservation can be performed either at the transmitting node or at the fusion node. Both cases will be studied. In the first two methods the consistency preservation is realized at the fusion node and in the other three methods it is made before transmission. The five methods are presented below.

A. Post-Transmission Adaption of Covariance Intersection

Given two estimates $(\hat{\mathbf{x}}_1, \mathbf{P}_1)$ and $(\hat{\mathbf{x}}_2, \mathbf{D}_2)$ of the same true state $\mathbf{x}$ to be fused, CI cannot be used directly since $\mathbf{D}_2$ is not necessarily consistent (if a consistent fused estimate must be guaranteed). However, each component $x_{2,i}$ of the n-dimensional estimate $\hat{\mathbf{x}}_2$ can be considered as a measurement of the i:th component of $\mathbf{x}$ with variance $\sigma_{2,i}^2$ equal to the i:th diagonal element of $\mathbf{D}_2$. These variances are consistent even though the cross-variances between components $i \neq j$ are unknown. An adaption of the CI algorithm can then be made, by collapsing the problem of fusing $\hat{\mathbf{x}}_1$ with one n-dimensional state $\hat{\mathbf{x}}_2$, to a problem of fusing $\hat{\mathbf{x}}_1$ with n one-dimensional state estimates $x_{2,i}$ of unknown cross-variances. Updating the CI equations given by (7), with $\mathbf{H}_1$ set to the identity matrix, in this case results in

$$\mathbf{P}_f^{-1} = \omega_1 \mathbf{P}_1^{-1} + \sum_{i=1}^{n} \omega_{2,i} \mathbf{H}_{2,i}^\intercal \sigma_{2,i}^{-2} \mathbf{H}_{2,i}, \tag{8a}$$

$$\mathbf{P}_f^{-1} \hat{\mathbf{x}}_f = \omega_1 \mathbf{P}_1^{-1} \hat{\mathbf{x}}_1 + \sum_{i=1}^{n} \omega_{2,i} \mathbf{H}_{2,i}^\intercal \sigma_{2,i}^{-2} x_{2,i}, \tag{8b}$$

where $\omega_1, \omega_{2,i} \in [0,1]$, $\omega_1 + \sum_{i=1}^{n} \omega_{2,i} = 1$ and the $1 \times n$ measurement matrices $\mathbf{H}_{2,i}$ are given by

$$\mathbf{H}_{2,i} = \begin{pmatrix} \delta_{i1} & \delta_{i2} & \ldots & \delta_{in} \end{pmatrix}, \tag{9}$$

with δ_{ij} being the *Kronecker delta*. The adapted version of CI, as given by (8) above, is a special case of CI as stated in Algorithm 1.

B. Uniform Post-Transmission Scaling

When node 1, the fusion node, receives $\mathbf{D} = \mathbf{D}_i$ from another node $i \neq 1$, node 1 does not know the original orientation and shape of the underlying matrix $\mathbf{P}$. This suggests that when node 1 handles $\mathbf{D}$, node 1 must assume that $\mathbf{P}$ can potentially be any covariance matrix that is bounded by the rectangular region illustrated in Fig. 1. Now, if for example the

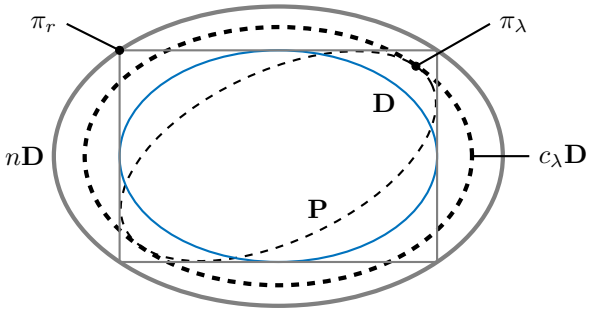

Fig. 1. The axis aligned ellipse within the rectangle, $\mathbf{D}$, is the diagonal covariance approximation of $\mathbf{P}$. $\mathbf{P}$ is represented by the dashed inclined ellipse. The matrix $n\mathbf{D}$ encloses the grey rectangle and will therefore enclose any possible matrix $\mathbf{P}$ with $\mathbf{D}$ defining the diagonal entries of $\mathbf{P}$. The covariance $c_\lambda\mathbf{D}$ is represented by the dashed ellipse that tangentially encloses $\mathbf{P}$.

point $\pi_r = (x_r, y_r)$ corresponding to the upper left corner of the rectangle in Fig. 1 is inserted into the axis aligned ellipse equation

$$\frac{1}{c}\frac{x_r^2}{\sigma_x^2} + \frac{1}{c}\frac{y_r^2}{\sigma_y^2} = \frac{1}{c} + \frac{1}{c} = 1, \tag{10}$$

the scaling factor $c = 2$ can be resolved, where in the first step of (10) $x_r/\sigma_x = 1$ and $y_r/\sigma_y = 1$ have been used. The same reasoning for the n-dimensional case using the generalized version of (10), that is,

$$1 = \frac{1}{c}\sum_{i=1}^{n}\frac{x_i^2}{\sigma_i^2}, \tag{11}$$

yields the scaling factor $c = n$, *i.e.* the scaling factor is equal to the number of dimensions. It shall be noted that the scaling $c = n$ refers to the scaling of the covariance matrix $\mathbf{D}$ itself, each axis of the resulting ellipsoid is scaled by $\sqrt{n}$. This approach scales $\mathbf{D}$ uniformly in the sense that each axis is scaled by the same factor c.

That consistency really is recovered by scaling with $c = n$ is proven in Theorem 1.

Theorem 1. *Let $\mathbf{P}$ be a covariance matrix of size $n \times n$ and $\mathbf{D}$ the diagonal covariance matrix obtained by putting all off-diagonal entries of $\mathbf{P}$ to zero. Then $n\mathbf{D} - \mathbf{P} \succeq 0$*

Proof. If $c\mathbf{D} - \mathbf{P} \succeq 0$, where c is a positive scalar and $\mathbf{D}$ and $\mathbf{P}$ are of size $n \times n$, the following is true

$$c\mathbf{D} - \mathbf{P} \succeq 0, \tag{12}$$
$$\iff c\mathbf{D}^{-\frac{1}{2}}\mathbf{D}\mathbf{D}^{-\frac{1}{2}} - \mathbf{D}^{-\frac{1}{2}}\mathbf{P}\mathbf{D}^{-\frac{1}{2}} \succeq 0, \tag{13}$$
$$\iff c\mathbf{I} - \mathbf{Q} \succeq 0, \tag{14}$$

where $\mathbf{I}$ is the identity matrix and $\mathbf{Q}$ is the correlation matrix having ones on its diagonal and the off-diagonal elements $i \neq j$ are bounded as $|q_{ij}| \leq 1$. Hence, choosing the dimensionality $c = n$ as the scaling constant, $n\mathbf{I} - \mathbf{Q}$ becomes a symmetric diagonally dominant matrix and we get $n\mathbf{I} - \mathbf{Q} \succeq 0 \iff n\mathbf{D} - \mathbf{P} \succeq 0$ [21]. □

C. Uniform Pre-Transmission Eigenvalue-Based Scaling

For obvious reasons the transmitter has more knowledge about the covariance matrix to be transmitted. A more information efficient scaling should therefore be possible if the scaling is performed at the transmitting node.

Geometrically, this approach is similar to the previous case. An eigenvalue analysis of $\mathbf{P}$ exploits the orientation and scaling in each direction of the covariance ellipsoid. By finding the largest eigenvalue and the corresponding eigenvector the point π_λ farthest from the center of the ellipsoid is retrieved. A co-centric and axis aligned ellipsoid $c_\lambda\mathbf{D}$ that tangents this point will precisely enclose $\mathbf{P}$. The ellipsoid $c_\lambda\mathbf{D}$, where the scaling factor c_λ is found by plugging π_λ into (11), is illustrated in two dimensions in Fig. 1.

The geometrically oriented argument above of finding c_λ is equivalent to Theorem 2. A desirable property of this eigenvalue-based scaling method is that $c_\lambda \gtrapprox 1$ in the case where the original covariance $\mathbf{P}$ is approximately axis aligned.

Theorem 2. *Let $\mathbf{P}$ be a covariance matrix and $\mathbf{D}$ the diagonal covariance matrix obtained by putting all off-diagonal entries of $\mathbf{P}$ to zero. Then $c_\lambda\mathbf{D} - \mathbf{P} \succeq 0$ where c_λ is the largest eigenvalue of the correlation matrix $\mathbf{Q} = \mathbf{D}^{-\frac{1}{2}}\mathbf{P}\mathbf{D}^{-\frac{1}{2}}$.*

Proof. We have $c\mathbf{D} - \mathbf{P} \succeq 0 \iff c\mathbf{I} - \mathbf{Q} \succeq 0$, where $\mathbf{Q} = \mathbf{D}^{-\frac{1}{2}}\mathbf{P}\mathbf{D}^{-\frac{1}{2}}$ and c is a scalar. $c\mathbf{I} - \mathbf{Q} \succeq 0$ is equivalent to

$$\mathbf{y}^\intercal\left(c\mathbf{I} - \sum_i \lambda_i\mathbf{v}_i\mathbf{v}_i^\intercal\right)\mathbf{y} \geq 0, \quad \forall\mathbf{y} \tag{15}$$

where $\mathbf{Q}$ has been replaced by its eigendecomposition. $\mathbf{v}_i$ is the eigenvector corresponding to eigenvalue λ_i. Further, $\mathbf{v}_i$ is normalized implying $\|\mathbf{y}^\intercal\mathbf{v}_i\| \leq \|\mathbf{y}\|$. Without loss of generality, assume $\|\mathbf{y}\| = 1$, and (15) reduces to

$$c - \sum_i \lambda_i\mathbf{y}^\intercal\mathbf{v}_i\mathbf{v}_i^\intercal\mathbf{y} \geq 0, \quad \forall\mathbf{y}, \|\mathbf{y}\| = 1 \tag{16}$$

which will be minimized by $\mathbf{y} = \mathbf{v}_1$ where $\mathbf{v}_1$ is the eigenvector corresponding to the maximum eigenvalue λ_1, *i.e.*

$$c - \sum_i \lambda_i\mathbf{v}_1^\intercal\mathbf{v}_i\mathbf{v}_i^\intercal\mathbf{v}_1 = c - \lambda_1 \geq 0. \tag{17}$$

By choosing $c = c_\lambda = \lambda_1$ we have $c_\lambda\mathbf{I} - \mathbf{Q} \succeq 0 \iff c_\lambda\mathbf{D} - \mathbf{P} \succeq 0$. □

D. Non-uniform Pre-Transmission Optimization-Based Scaling

The scaling problem can also be formulated as an optimization problem. Let $\mathbf{c} = (c_1, \ldots, c_n)$ denote the vector of scaling

factors where each element $c_i \geq 1$. Construct the matrices $\mathbf{C} = \text{diag}(\mathbf{c})$ and $\mathbf{D}_c = \mathbf{CD}$, and solve

$$\begin{aligned} \underset{\mathbf{c}}{\text{minimize}} \quad & f(\mathbf{D}_c(\mathbf{c})) \\ \text{subject to} \quad & \mathbf{D}_c - \mathbf{P} \succeq 0. \end{aligned}$$

$\mathbf{D}_c$ will generally be scaled non-uniformly. Solving for $\mathbf{D}_c$ yields the optimal diagonal matrix, based on the particular objective function f, that preserves consistency according to the constraint. The trace is here used as f.

E. Non-uniform Pre-Transmission Diagonal-Dominance Scaling

The proof of Theorem 1 illuminates diagonal dominance and its relationship to positive (semi)-definiteness which suggests the following argument. If a diagonal matrix $\mathbf{D}$ is constructed, where the i:th diagonal entry of $\mathbf{D}$ is the absolute sum of row i of $\mathbf{P}$, *i.e.*

$$d_{ii} = \sum_j |p_{ij}|, \tag{18}$$

then $\mathbf{D} - \mathbf{P}$ will automatically be a symmetric diagonally dominant matrix and as such be positive semi-definite [21].

V. Experimental Evaluation

To compare the consistency preservation capability and performance of the different methods computer simulations will be made. The following consistency preserving methods will be considered (the emphases refer to the naming of the corresponding method):

1) *CI adapted* – CI with an adaption to handle the diagonal covariance approximation (Sec. IV-A)
2) *CI dim-scale* – CI with uniform dimension-based post-transmission scaling of $\mathbf{D}$ (Sec. IV-B)
3) *CI eigen-scale* – CI with eigenvalue-based pre-transmission scaling of $\mathbf{D}$ (Sec. IV-C)
4) *CI opt-scale* – CI with non-uniform optimization-based pre-transmission scaling of $\mathbf{D}$ (Sec. IV-D)
5) *CI diag-dom-scale* – CI with diagonal-dominance pre-transmission scaling of $\mathbf{D}$ (Sec. IV-E)

As references, the cases below will also be considered:

6) *CI full P* – CI with complete covariance $\mathbf{P}$
7) *LKF* – local KF with access to only local information
8) *CKF* – centralized KF with access to the complete information (measurements including covariance) from all nodes
9) *nKF* – naïve KF with access to network complete covariance $\mathbf{P}$

A. Simulation Scenario

The dynamic scenario used for evaluation is illustrated in Fig. 2. Two aircraft (A and B) are approaching aircraft C from south at a speed of 100 m/s. A and B are separated by 10 km and are initially 20 km south of C. C follows the dashed trajectory at a speed of 200 m/s. A and B have each a tracking sensor of high bearing accuracy but poor range accuracy. A and B can also exchange information with each other, but not with C, via a datalink.

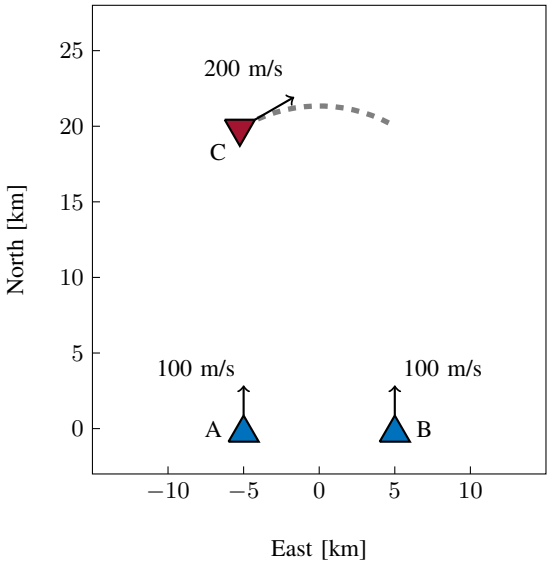

Fig. 2. The simulated scenario. Two aircraft A and B follow parallel straight trajectories and approach aircraft C from south. C follows the dashed trajectory.

The simulations are performed in 3D using a north-east-down (NED) coordinate frame. The state vector comprising both position and velocity is of 6D. The true motions are confined to a constant altitude. All filters considered use a *constant velocity* model for the time update with the process noise parameter σ_w tuned such that consistent estimates are generated by the CKF. The range, elevation and azimuth uncertainties of the tracking sensor are modelled as $\sigma_r = 1000\,\text{m}$, $\sigma_\theta = 0.1^\circ$ and $\sigma_\phi = 0.1^\circ$, respectively.

The tracking sensor in each of the aircraft A and B scans the tracking volume and generates new measurements of C at a rate of approximately 0.7 Hz. A converted measurements KF is used to fuse the tracking sensor measurements with the track, where the measurement covariance matrix in NED is calculated by converting the original covariance matrix, which is a diagonal covariance matrix in spherical coordinates, to cartesian coordinates followed by a rotation and subsequent translation into the NED frame. The probability of detection is set to 100% and a clutter free environment is assumed. The transmission rate of the datalink is 1 Hz.

A *Monte Carlo* (MC) simulation approach is considered in MATLAB® with 100 MC runs for each method. Each MC run is of 20 s. The optimization problems, introduced by CI adapted and CI opt-scale, are solved using `YALMIP` [22].

B. Performance and Consistency Evaluation

The proposed methods are evaluated both on their performance and their credibility. The performance of each method is evaluated using the *root mean squared error* (RMSE) as ground truth is available. To have a meaningful physical interpretation of the RMSE the state vector is divided into

its position and velocity components, giving RMSE_P and RMSE_V, respectively. RMSE can both be calculated for all time points during one MC run or as the RMSE for one specific time point over all MC runs. The latter will be used here.

The level of consistency of each method is evaluated by calculating the statistical measure *normalized estimation error squared* (NEES) defined as [23]

$$\varepsilon(k) = (\mathbf{x}(k) - \hat{\mathbf{x}}_f(k|k))^\intercal \mathbf{P}_f^{-1}(k|k)(\mathbf{x}(k) - \hat{\mathbf{x}}_f(k|k)), \quad (19)$$

where $(\hat{\mathbf{x}}_f, \mathbf{P}_f)$ is the fused estimate and k is the time index. As M number of MC simulations are performed multiple values of $\varepsilon_i(k)$ for each time point k are generated. From these the *average NEES* (ANEES) at each time point k can be calculated as [24]

$$\bar{\varepsilon}(k) = \frac{1}{nM} \sum_{i=1}^{M} \varepsilon_i(k), \quad (20)$$

i.e. ANEES is simply NEES averaged over the MC runs and normalized using the dimensionality n. A fusion rule providing ANEES significantly lower than 1 is regarded as consistent but conservative. A fusion rule providing ANEES significantly higher than 1, above is regarded as too optimistic and inconsistent.

Confidence intervals for ANEES are derived in [24] and are calculated, for $nM \gg 5$, as

$$\left[\left(c - p\sqrt{\frac{2}{9nM}} \right)^3, \left(c + p\sqrt{\frac{2}{9nM}} \right)^3 \right], \quad (21)$$

where $c = 1 - 2/9nM$ and p depends on the confidence level, *e.g.* $p = 1.96$ and $p = 2.576$ for 95% and 99% confidence levels, respectively.

C. Results and Discussion

In Fig. 3 ANEES over the MC simulations is presented. All methods, except the nKF (and initially the LKF), lie below the CKF reference and the solid line at ANEES equal to 1 indicating they provide consistent estimates throughout the simulation time. CI adapted, CI eigen-scale, CI opt-scale and CI diag-dom-scale are the most conservative methods giving an ANEES of about 0.3–0.5. Even though CI dim-scale produces the largest upscaled covariance of the scaling-oriented methods it is still slightly less conservative than CI adapted, CI eigen-scale, CI opt-scale and CI diag-dom-scale.

With the exception of nKF (see Fig. 4) the RMSE_P of all methods is bounded from below by CKF and from above by LKF. The optimistic nKF severely underestimates the fused covariance leading to that the estimates diverge rather quickly. Of the proposed methods CI dim-scale performs the worst, presumably because the systematically and excessively up-scaling of $\mathbf{D}$ is followed by a substantial loss of information. Because of the relatively high update rate of the datalink, CI full P quickly approaches the CKF. The RMSE_V counterpart to Fig. 4 is given in Fig. 5. Because of the constant speed of

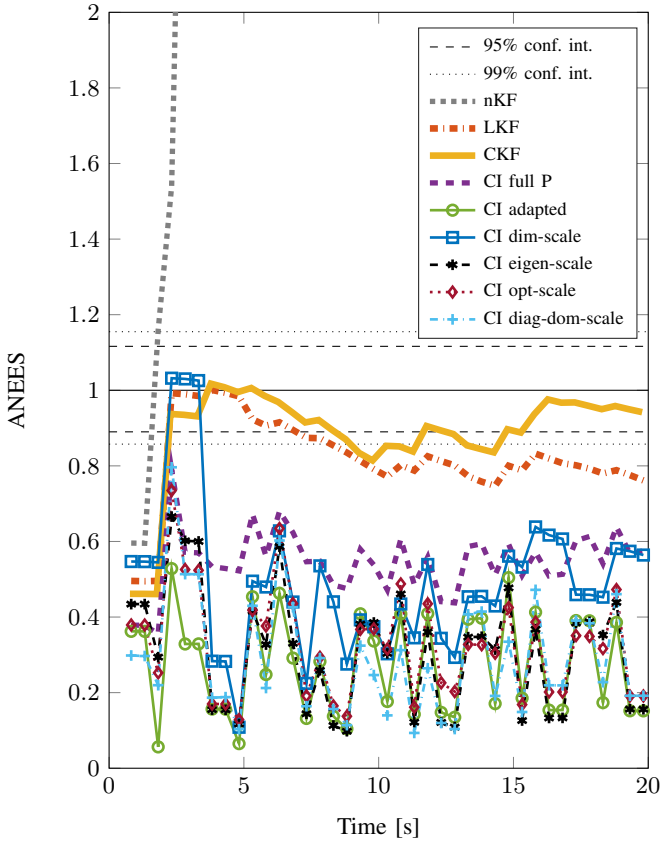

Fig. 3. ANEES vs elapsed time since start of simulation. 95% and 99% confidence intervals for ANEES are also shown.

tracked target the RMSE_V converges relatively quickly for all methods.

To resolve the multiple curves illustrated in Fig. 3, 4 and 5, Table I has been provided. Table I summarizes each curve into a single value by simply taking the mean over all time points.

It is interesting to note that not only CI eigen-scale, CI opt-scale and CI diag-dom-scale, but also CI adapted, provide approximately the same results, even though they are derived from different aspects. One explanation of CI eigen-scale and CI opt-scale being very close in both performance (RMSE) and consistency (ANEES) is that the optimization method in fact finds the same scaled diagonal covariance matrix as do the eigenvalue-based scaling approach as its optimization solution. CI adapted being so close to CI eigen-scale, CI opt-scale and CI diag-dom-scale is beneficial for practical reasons, a platform operating in a network having a communication protocol constrained as dealt with herein can simply post-transmission fix the inconsistency of the received diagonal covariance matrix by CI adaption. One drawback is however that CI adapted involves solving a computational expensive optimization problem, similar to CI opt-scale, which is not the case for CI eigen-scale.

The required bandwidth in case of transmission of the full estimate $(\hat{\mathbf{x}}, \mathbf{P})$ scales as $n + n(n+1)/2 = n(n+3)/2$, where

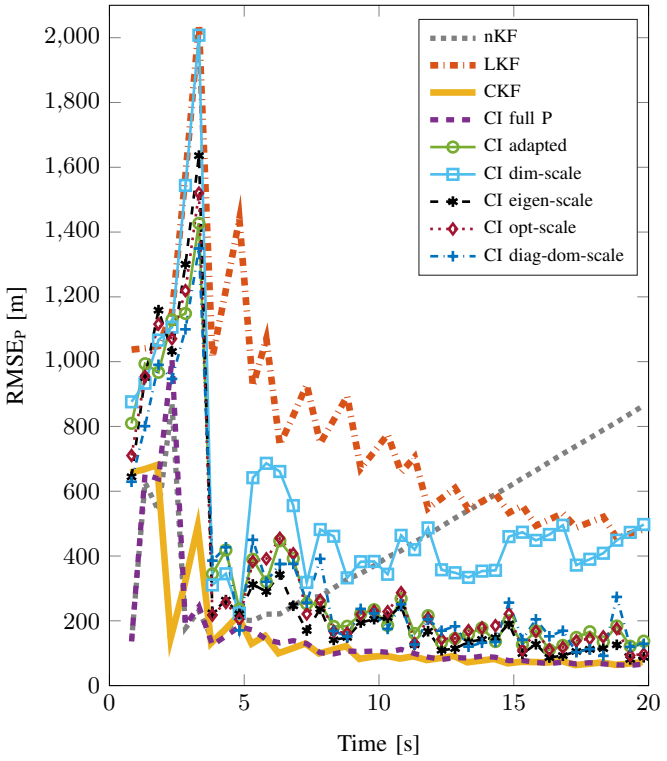

Fig. 4. RMSE$_P$ vs elapsed time since start of simulation.

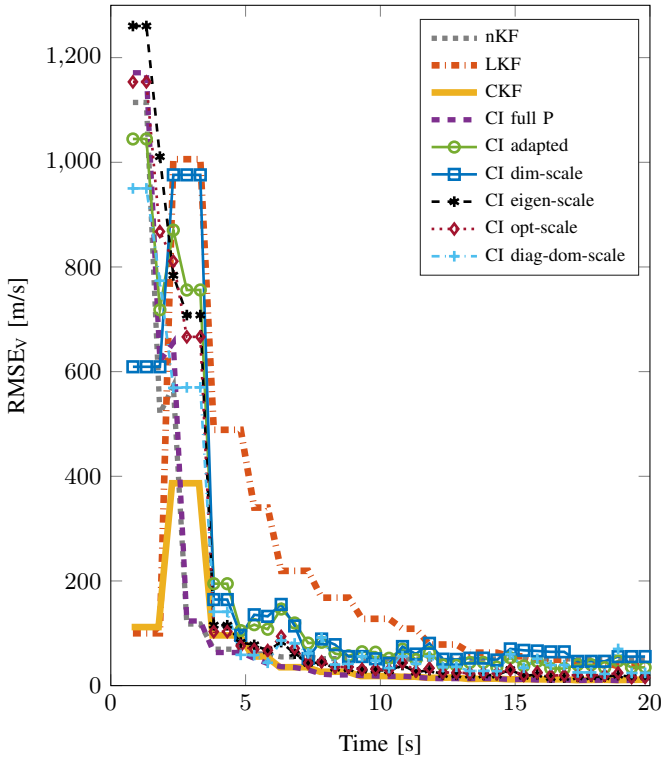

Fig. 5. RMSE$_V$ vs elapsed time since start of simulation.

n is the number of dimensions, assuming a uniform bit depth for all variables. For the diagonal covariance approximation $(\hat{\mathbf{x}}, \mathbf{D})$ the required bandwidth for transmission of one estimates scales with dimensionality as $2n$.

It shall also be noted that a direct implementation of the CU method was evaluated without regarding that in our case we knew which of the estimates to be fused that were inconsistent. The performance however, was very poor and the direct CU implementation is therefore not presented and evaluated further here.

VI. Conclusions and Future Work

In this paper different consistency preserving methods for distributed track fusion have been evaluated with respect to their performance and consistency in dealing with the communication constraint implied by only being able to exchange the diagonal covariance approximation in place of the full covariance matrix.

The proposed methods were used in conjunction with the *covariance intersection* (CI) algorithm. As CI requires that all ingoing estimates are consistent for guaranteeing the fused estimate being consistent, different methods for consistency recovery were developed. Of the four proposed methods *CI adapted*, *CI eigen-scale*, *CI opt-scale* and *CI diag-dom-scale* performed equally well both with respect to the *root mean squared error* (RMSE) performance metric and the *average normalized estimation error squared* (ANEES) consistency metric. On the other hand, CI dim-scale showed a significantly worse performance with respect to RMSE, but with a ANEES closer to the optimal value 1. A remarkable result for practical applications is that CI adapted is able to perform equally well as CI eigen-scale, CI opt-scale and CI diag-dom-scale, even though the consistency recovery is made post-transmission at the fusion node where full information about the original covariance $\mathbf{P}$ is not available. Further, the primary advantage of CI diag-dom-scale is that it is very simple and straightforward to implement.

Another way of looking at the results is from a bandwidth consumption perspective. If handled carefully, the diagonal covariance approximation can considerably reduce the amount of data transmitted while still being both consistent and able of performing well in an RMSE sense. This is of importance in many real-world applications where sensor networks are required to act efficiently both in terms of communication (bandwidth) and performance.

The next step is to investigate how the different proposed methods scales with the number of network nodes and to develop approximations if the scaling is not favourable. Also, the proposed methods should be implemented in conjunction with other distributed fusion schemes.

References

[1] S. J. Julier and J. K. Uhlmann, "A non-divergent estimation algorithm in the presence of unknown correlations," in *Proceedings of the 1997 American Control Conference (Cat. No.97CH36041)*, vol. 4, Jun. 1997, pp. 2369–2373.

[2] X. Tian and Y. Bar-Shalom, "Exact algorithms for four track-to-track fusion configurations: All you wanted to know but were afraid to ask," in *Proceedings of 12th IEEE International Conference on Information Fusion*, Seattle, WA, Jul. 2009.

TABLE I
THE MEAN OF EACH OF THE CURVES FOR ANEES, RMSE_P AND RMSE_V CALCULATED AS THE SAMPLE MEAN OVER ALL TIME POINTS.

	nKF	**LK**	**CKF**	**CI full P**	**CI adapted**	**CI dim-scale**	**CI eigen-scale**	**CI opt-scale**	**CI diag-dom-scale**
ANEES	3 980	0.820	0.885	0.547	0.270	0.497	0.303	0.319	0.290
RMSE_P [m]	493	785	154	179	352	559	322	346	342
RMSE_V [m/s]	137	206	59	118	189	182	174	166	153

[3] Y. Bar-Shalom and L. Campo, "The effect of the common process noise on the two-sensor fused-track covariance," *IEEE Trans. Aerosp. Electron. Syst.*, vol. AES-22, no. 6, pp. 803–805, Nov. 1986.

[4] K. C. Chang, R. K. Saha, and Y. Bar-Shalom, "On optimal track-to-track fusion," *IEEE Trans. Aerosp. Electron. Syst.*, vol. 33, no. 4, pp. 1271–1276, Oct. 1997.

[5] L. Y. Pao and M. Kalandros, "Algorithms for a class of distributed architecture tracking," in *Proceedings of the 1997 American Control Conference (Cat. No.97CH36041)*, vol. 3, Jun. 1997, pp. 1434–1438.

[6] S. P. McLaughlin, R. Evans, and V. Krishnamurthy, "Data incest removal in a survivable estimation fusion architecture," in *Proceedings of the 6th International Conference on Information Fusion, FUSION 2003*, vol. 1, 02 2003, pp. 229–236.

[7] S. McLaughlin, V. Krishnamurthy, and S. Challa, "Managing data incest in a distributed sensor network," in *2003 IEEE International Conference on Acoustics, Speech, and Signal Processing, 2003. Proceedings. (ICASSP '03).*, vol. 5, Apr. 2003, pp. V–269.

[8] M. Reinhardt, B. Noack, M. Baum, and U. D. Hanebeck, "Analysis of set-theoretic and stochastic models for fusion under unknown correlations," in *14th International Conference on Information Fusion*, Jul. 2011, pp. 1–8.

[9] L. M. Kaplan, W. D. Blair, and Y. Bar-Shalom, "Simulations studies of multisensor track association and fusion methods," in *2006 IEEE Aerospace Conference*, Mar. 2006.

[10] S. J. Julier and J. K. Uhlmann, *Handbook of Multisensor Data Fusion*. Boca Raton, FL: CRC Press, 2001, ch. General Decentralized Data Fusion with Covariance Intersection.

[11] A. R. Benaskeur, "Consistent fusion of correlated data sources," in *IEEE 2002 28th Annual Conference of the Industrial Electronics Society. IECON 02*, vol. 4, Nov. 2002, pp. 2652–2656.

[12] J. Sijs, M. Lazar, and P. P. J. v. d. Bosch, "State fusion with unknown correlation: Ellipsoidal intersection," in *Proceedings of the 2010 American Control Conference*, Jun. 2010, pp. 3992–3997.

[13] J. Sijs and M. Lazar, "Empirical case-studies of state fusion via ellipsoidal intersection," in *14th International Conference on Information Fusion*, Jul. 2011, pp. 1–8.

[14] J. Nygårds, V. Deleskog, and G. Hendeby, "Safe fusion compared to established distributed fusion methods," in *Proceedings of IEEE Int. Conf. on Multisensor Fusion*, Baden-Baden, Germany, Sep. 2016.

[15] B. Noack, J. Sijs, M. Reinhardt, and U. D. Hanebeck, "Decentralized data fusion with inverse covariance intersection," *Automatica*, vol. 79, pp. 35–41, May 2017.

[16] B. Noack, J. Sijs, and U. D. Hanebeck, "Inverse covariance intersection: New insights and properties," in *Proceedings of 20th IEEE International Conference on Information Fusion*, Xi'an, China, Jul. 10–13 2017.

[17] J. Nygårds, V. Deleskog, and G. Hendeby, "Decentralized tracking in sensor networks with varying coverage," in *Proceedings of 21th IEEE International Conference on Information Fusion*, Cambridge, UK, Jul. 10–13 2018.

[18] J. Ajgl and O. Straka, "A geometrical perspective on fusion under unknown correlations based on minkowski sums," in *2017 20th International Conference on Information Fusion (Fusion)*, July 2017, pp. 1–8.

[19] J. K. Uhlmann, "Covariance consistency methods for fault-tolerant distributed data fusion," *Information Fusion*, vol. 4, pp. 201–215, Sep. 2003.

[20] T. Kailath, A. H. Sayed, and B. Hassibi, *Linear Estimation*. New Jersey: Prentice Hall, 2000.

[21] R. A. Horn and C. R. Johnson, *Matrix Analysis*, 2nd ed. New York, NY, USA: Cambridge University Press, 2012.

[22] J. Löfberg, "Yalmip: A toolbox for modeling and optimization in matlab," in *Proceedings of the CACSD Conference*, vol. 3. Taipei, Taiwan, 2004.

[23] Y. Bar-Shalom, X. Li, and T. Kirubarajan, *Estimation with Applications to Tracking and Navigation: Theory Algorithms and Software*. Wiley & Sons, 2004.

[24] X. Rong Li, Z. Zhao, and V. P. Jilkov, "Practical measures and test for credibility of an estimator," Jan. 2001.